Accepted manuscript doi:
10.1680/jgeot.17.P.148

Accepted manuscript
As a service to our authors and readers, we are putting peer-reviewed accepted manuscripts (AM) online, in the Ahead of Print section of each journal web page, shortly after acceptance.

Disclaimer
The AM is yet to be copyedited and formatted in journal house style but can still be read and referenced by quoting its unique reference number, the digital object identifier (DOI). Once the AM has been typeset, an 'uncorrected proof' PDF will replace the 'accepted manuscript' PDF. These formatted articles may still be corrected by the authors. During the Production process, errors may be discovered which could affect the content, and all legal disclaimers that apply to the journal relate to these versions also.

Version of record
The final edited article will be published in PDF and HTML and will contain all author corrections and is considered the version of record. Authors wishing to reference an article published Ahead of Print should quote its DOI. When an issue becomes available, queuing Ahead of Print articles will move to that issue's Table of Contents. When the article is published in a journal issue, the full reference should be cited in addition to the DOI.

Downloaded by [TU Delft Library] on [10/10/18]. Copyright © ICE Publishing, all rights reserved.

Accepted manuscript doi:
10.1680/jgeot.17.P.148

Submitted: 06 June 2017

Published online in 'accepted manuscript' format: 18 September 2018

Manuscript title: Experimental results on the influence of gas on the mechanical response of peats

Authors: Cristina Jommi*[†], Stefano Muraro*, Edoardo Trivellato*[‡] and Cor Zwanenburg[§]

Affiliations: *Department of Geoscience and Engineering, Delft University of Technology, Stevinweg 1, 2628 CN Delft, The Netherlands; [†]Department of Civil and Environmental Engineering, Politecnico di Milano, piazza Leonardo da Vinci 32, 20133 Milano, Italy; [‡]presently: Ecole Nationale des Ponts et Chaussées (Ecole des Ponts ParisTech) - Laboratoire Navier, Champs sur Marne and [§]Deltares, Delft, The Netherlands

Corresponding author: Cristina Jommi, Department of Geoscience and Engineering, Delft University of Technology, Stevinweg 1 , 2628 CN Delft, The Netherlands. Tel. +31 15 27 84173.

E-mail: C.Jommi@tudelft.nl

Downloaded by [TU Delft Library] on [10/10/18]. Copyright © ICE Publishing, all rights reserved.

Accepted manuscript doi:
10.1680/jgeot.17.P.148

Abstract

Direct observation of gas in peat layers, generated by slow degradation in anoxic conditions, raised concern in the Netherlands about its potential impact on the geotechnical response of dykes founded on peat. To address this issue, an experimental investigation was initiated aimed at quantifying the main consequences of the presence of gas on the mechanical response of peats. The results of a series of triaxial tests on natural peat samples flushed with carbonated water are presented and discussed. Controlled amounts of gas were exsolved by undrained isotropic unloading, and the samples were sheared under undrained conditions. During gas exsolution, the samples suffered volumetric expansion, at a rate which is ruled by the relative compressibility of the fluid and the soil skeleton. The gas in the pore fluid dominates the stress-strain response upon undrained shearing, causing lower excess pore pressure compared to fully saturated samples. The experimental results suggest that local fabric changes occur during gas exsolution. However, for the amounts of gas investigated, these fabric changes seem to be almost reversible upon compression. Although the ultimate shear strength is hardly affected by gas, the reduction in the mobilised shear strength at given axial strain thresholds is dramatic, compared to fully saturated samples. The study suggests that the presence of gas must be cautiously accounted for at low stresses, when a reference stiffness is chosen for serviceability limit states, and when operative shear strength definitions, based on mobilised strength for given strain thresholds, are chosen in the assessment of geotechnical structures on peats.

Keywords: Organic soil; Gassy soil; Laboratory tests; Shear strength; Compressibility

Downloaded by [TU Delft Library] on [10/10/18]. Copyright © ICE Publishing, all rights reserved.

Accepted manuscript doi:
10.1680/jgeot.17.P.148

INTRODUCTION AND MOTIVATION

Many flood defence embankments in the Netherlands have been built on peat layers - dykes on peat - or are made of peat - peat dykes. The assessment of these dykes is not straightforward, especially due to the lack of adequate geotechnical description of the behaviour of peats at the engineering scale. This often results in very prudential assumptions, leading to high costs for maintenance and reinforcement. Several difficulties arise from the peculiar characteristics of this material, such as the exceptional high water content up to 800% - 900% and the organic content reaching 80% - 90%, multiple levels of fibrous structures and creep behaviour. Among these aspects, concerns on the stability and the serviceability of these dykes also arise from biodegradation of peat.

Oxidation of the organic fraction leads to significant modification of the soil skeleton compressibility, strength and retention capacity. In addition, the decomposition of organic matter produces gas species, typically CO_2 in aerobic environment and H_2S and CH_4 in deeper peat layers under anaerobic conditions. Dissolution of the available free gas and continuous degradation of the organic matter tend to saturate the pore fluid with gases. These are exsolved in the form of gas bubbles when their concentration exceeds the equilibrium solubility, because of atmospheric pressure changes, temperature oscillations, water table drop or total stress reduction (Dinel et al., 1988; Brown et al., 1989; Buttler et al., 1991). Previous research has addressed the role played by biogenic gas on buoyancy, retention, hydraulic conductivity, and volumetric expansion and contraction of peats, mostly from a hydrological perspective (Kellner et al., 2004, 2005; Waddington et al., 2009; Rosenberry et al., 2003; Tokida et al., 2005; Tokida et al., 2007; Glaser et al., 2004; Strack et al., 2005). Only few contributions dealt with the possible geotechnical impact of gas in peats with reference to the structural response of dykes or railway embankments (Vonk, 1994; Den

Downloaded by [TU Delft Library] on [10/10/18]. Copyright © ICE Publishing, all rights reserved.

Accepted manuscript doi:
10.1680/jgeot.17.P.148

Haan & Kruse, 2007; Acharya et al., 2016a, 2016b). However, all these contributions just highlighted that local overpressure may occur due to gas pockets, but none of them included a systematic study on the consequences of gas entrapment on the mechanical behaviour of peats.

The effects of entrapped gas have been studied extensively in the past for marine sands and clays (e.g. Nageswaran, 1983; Wheeler, 1988a; Rad et al., 1994; Grozic et al., 1999; Grozic et al., 2000; Hight & Leroueil, 2003; Sultan et al., 2007; Amaratunga & Grozic, 2009; Sultan et al., 2012). In the case of sands, it is recognised that the predominant effect of gas is to increase the pore fluid compressibility, which affects the pore pressure development during shear, in turn increasing or decreasing the ultimate shear strength depending on the relative density of the sand (Rad et al., 1994; Grozic et al., 1999; Grozic et al., 2000). More controversial results were found on clays, because of the role played by two competing mechanisms, depending on the combination of total stress and water pressure. On the one hand, the reduction in the fluid stiffness increases the mean effective stress and has a positive influence on the attainable undrained shear strength (Wheeler, 1988a; Grozic et al., 2005). However, the increase in the gas pressure during exsolution may damage the pore structure, and the formation of large gas filled pores eventually has a negative impact on the available shear strength (Nageswaran, 1983; Hight & Leroueil, 2003; Sultan et al., 2012).

Attention was raised on the influence of biogenic gas on the geotechnical response of flood defences in the Netherlands during a thorough field study of dykes founded on peat, where gas release was regularly observed (Zwanenburg, 2013). As the lack of systematic studies on the mechanical response of gassy peats increases the knowledge uncertainties on the short-term performance and the long-term durability of the embankments, an experimental investigation was initiated at TU Delft to start filling the knowledge gap (Jommi et al., 2017).

Downloaded by [TU Delft Library] on [10/10/18]. Copyright © ICE Publishing, all rights reserved.

Accepted manuscript doi:
10.1680/jgeot.17.P.148

To isolate the mechanical effects of gas on the soil skeleton from the direct consequences of biodegradation of the material, a series of triaxial compression tests has been performed on intact peat samples artificially charged with a controlled amount of gas. Some of the implications of the presence of gas in peat are discussed from the results of the triaxial compression tests, where attention has been given to the impact of gas on both volumetric and deviatoric response. The testing programme was designed to provide an answer to the following questions: (i) how will the pore fluid pressure and the average stress acting on the soil skeleton be affected by the generation of gas? (ii) is the amount of exsolved and entrapped gas dependent on the soil skeleton properties and on the external confinement? (iii) will the gas volume and pressure affect the fabric of peat and will the modification be irreversible in this case? (iv) how will the deviatoric response be affected by gas, and will ultimate shear strength depend on the amount of gas?

EXPERIMENTAL PROGRAMME

Material

The experimental study has been conducted on undisturbed peat specimens sampled between -1.0 and -2.5 m depth from the ground level in the subsoil of the Markermeer dykes at Katwoude in the Netherlands (De Vries & De Bruijn, 2014). The soil profile is made of a 0.7 - 1 m thick silty clay cover above a peat layer with a variable thickness of 2 - 3 m, where the samples were retrieved. The water table is located 0.25 m below the ground level. The in situ effective vertical stress of the peat layer is around 10 kPa, typical of surficial peat layers in the Netherlands. After sampling, the material was stored in a climate controlled room at 10°C and 90% relative humidity to prevent oxidation of the organic matter. The water content was determined by oven drying at 60°C to avoid loss of organic mass (Head, 2014). The specific gravity of the soil, Gs, was measured with a helium pycnometer in accordance to

Downloaded by [TU Delft Library] on [10/10/18]. Copyright © ICE Publishing, all rights reserved.

Accepted manuscript doi:
10.1680/jgeot.17.P.148

ASTM D5550–14 (ASTM, 2014a) and the organic content was assessed by ignition at 500°C (ASTM, 2014b; Den Haan & Kruse, 2007).

Table 1 reports the index properties of the tested samples. Three tests assessing loss of ignition (N) following the standard ASTM D2974-14 (ASTM, 2014b) gave an average organic content OC of 85.7% based on relation (1) (Skempton & Petley, 1970)

$$1 - \mathrm{OC} = 1.04(1 - \mathrm{N}) \, . \qquad (1)$$

The data reported in the table show that the soil in the field is not completely saturated and that, on average, the lower the degree of decomposition (smaller values of specific gravity) the lower the in situ degree of saturation.

Experimental set-up and procedure

A series of triaxial tests was carried out on samples 100 mm in height and 50 mm in diameter. A load frame type GDS triaxial system with standard back pressure and cell pressure volume controllers and a submersible 1 kN load cell was used (Fig. 1). The accuracy of the controllers is ± 1 kPa on pressure and ± 300 mm^3 on volume (0.15% FSR). Calibration of the system included the cell deformation during loading and unloading at the pressures used in the tests, using a steel sample replica. The calibration was essential to allow using the variations in volume recorded by the cell pressure volume controller, together with the volume change due to the piston displacement, to compute the volumetric strain of the sample, ε_p, during the undrained unloading (gas exsolution and expansion) and during the next shearing stage (gas compression and dissolution).

All the tests were performed in a controlled environment, at temperature T = 13 °C and relative humidity RH = 68%. Carbonated water was prepared before each test in a Perspex cell, where CO_2 dissolution in de-aired water at a target pressure of 380 kPa was allowed for about 60 hours at 22 °C (Van der Putte, 2014).

Downloaded by [TU Delft Library] on [10/10/18]. Copyright © ICE Publishing, all rights reserved.

Accepted manuscript doi:
10.1680/jgeot.17.P.148

To generate a controlled amount of gas in the peat samples, the protocol suggested by Lunne et al. (2001), Amaratunga & Grozic (2009) and Sultan et al. (2012) was followed. After mounting in the triaxial apparatus, the samples were loaded isotropically to a cell pressure of about 400 kPa under undrained conditions, to dissolve the natural gas and air bubbles in the peat samples. Afterwards, the pore water was replaced with carbonated water, by flushing the samples from a third pressure controller connected to the pedestal (Fig. 1). A total volume of about 1.3 times the initial volume of voids was injected, under a small pressure difference of 2 - 4 kPa between the bottom and the top cap. Flushing was performed under a total isotropic stress between 400 and 420 kPa, while the effective confining mean stress ranged between 5 - 15 kPa. Before exsolving the gas previously injected in the samples, the effective stress was increased with a first short isotropic consolidation stage. Gas exsolution was triggered by decreasing the isotropic confining pressure under external undrained conditions. A second isotropic consolidation stage was performed on the gassy samples in order to re-adjust the confining stress to the target value after the gas exsolution, before the start of shearing.

Undrained shearing was performed at controlled axial displacement rate of 0.02 mm/min, to replicate the one adopted in a previous extensive experimental study on saturated samples of peat coming from the same Markermeer area (De Vries & de Bruijn, 2014). As the behaviour of peat is rate sensitive, the same displacement rate was chosen to minimise the differences in the stress-strain response coming from rate dependency, and to allow isolating and evaluating the role played by the gas. However, in Test 6, stress controlled shearing was chosen to check the controllability of the mechanical response, which implied a variable strain rate, on average about five times higher than that experienced by the other samples. To limit gas diffusion from the samples, two latex membranes 0.25 mm thick with an intermediate grease layer in between were used. The choice seems to be substantiated by the results from sample

Downloaded by [TU Delft Library] on [10/10/18]. Copyright © ICE Publishing, all rights reserved.

Accepted manuscript doi:
10.1680/jgeot.17.P.148

6, which was sheared five times faster than the others, though experiencing comparable volumetric strain.

A reference test was performed on a sample fully saturated with demineralized de-aired water (Test 1). A second reference sample was tested after flushing with demineralised water saturated with nitrogen N_2 (Test 2). Flushing with N_2 charged water, allowed removing the small amount of oxygen that can remain in water even after de-airing process with a standard pump, and provides an alternative convenient reference for saturated conditions. Flushing was performed also for the saturated samples to minimise the differences in fabric changes between different samples, which could be due just to the saturation procedure.

In Table 2 and Table 3 the cell pressure (σ_c), the back pressure (u_b) and the pore fluid pressure measured at the bottom of the sample (u_f) are reported for each sample, for the different stages of the tests, until the start of shearing. It is worthwhile noting that the mean effective stress in the field can be estimated to be around 7 kPa. The confining stresses attained in the triaxial apparatus were slightly higher than the latter, to improve the accuracy of the results, still being representative of the site conditions.

EXPERIMENTAL RESULTS

Describing and interpreting the stress-strain response of gassy peat samples requires making a choice on the most convenient stress variables to be used in the description of the results. The choice is not straightforward in the case of this experimental investigation, as the samples experience different states during the triaxial tests. At the start of the test, the peat is saturated with an almost incompressible fluid. Gas starts to be exsolved in the form of small bubbles, which are still surrounded by water. In these first two states, the measured pore pressure is the water pressure, and the solid skeleton response is likely to depend on the traditional effective stress, defined as the difference between the total stress and the water pressure. At

Downloaded by [TU Delft Library] on [10/10/18]. Copyright © ICE Publishing, all rights reserved.

Accepted manuscript doi:
10.1680/jgeot.17.P.148

increasing volume, the gas starts acting directly on the solid skeleton, and the mechanical response of the soil samples will start depending on both gas and water pressures. The latter state calls for a description of the soil state accounting explicitly for the volume fraction of gas and for the unsaturated state of the soil. Different choices could be equally made in the latter case, mostly depending on the available experimental information (see, e.g. Gens, 1996).

In previous investigations on gassy soils, the difference between total stress and water pressure has been used for any gas volume fraction. However, concern has been raised about the extension of the effective stress principle to the gassy state, which motivated naming "operative stress" the adopted stress variable (Sills et al., 1991; Sills & Gonzalez, 2001). In this work, it was assumed that the pressure measured at the bottom transducer is the average fluid pressure acting on the soil skeleton, and that the difference between the total stress and the measured pressure can be conveniently adopted to describe the relevant characteristics of the soil mechanical response. However, it is not proven that this difference can be identified with an effective stress, which alone would rule entirely the soil response (Jommi, 2000). For this reason, the definition "operative stress" is maintained in the presentation of the results. Accordingly, the mean operative stress is defined as

$$p'' = p - u_f = \frac{\sigma''_a + 2\sigma''_r}{3} \tag{2}$$

where p is the total mean stress and σ''_a and σ''_r are the operative axial and radial stresses computed as difference between the axial and radial total stresses and the measured pore fluid pressure, u_f. In equation (2) the double apostrophe $''$ is used to mark the conceptual

Downloaded by [TU Delft Library] on [10/10/18]. Copyright © ICE Publishing, all rights reserved.

Accepted manuscript doi:
10.1680/jgeot.17.P.148

difference between effective and operative stress for the case of gassy soils (Sills et al., 1991).

Isotropic undrained unloading

The experimental results during the isotropic undrained unloading stage are reported in Fig. 2. Normalised cell pressure was obtained by dividing the current cell pressure with the correspondent value at the start of unloading, $\sigma_{c0,u}$. Reduction of the cell pressure to about 50 kPa (Table 2 and Table 3) was conducted in 2 hours for Test 1, Test 2 and Test 6, 4 hours for Test 4 and 5, while a slower step-by-step procedure was adopted in Test 3.

Based on the volumetric strains recorded in the tested gassy samples at the end of the unloading, the gas content attained a volumetric fraction between 4% and 16% with respect to the initial sample volume. These values replicated the average gas volumetric fraction often encountered in peat layers (Landva & Pheeney, 1980; Reynolds et al., 1992; Beckwith & Baird, 2001 and Baird & Waldron, 2003). As expected, fully saturated samples, Test 1 and Test 2, experienced null volumetric strains. The rate at which the pore fluid pressure decreases during unloading is ruled by gas exsolution and expansion (Sobkowicz & Morgenstern, 1984), which are expected to start when the pore fluid pressure drops below the initial gas-liquid saturation pressure, $u_{l/g,0}$. The detail of the evolution of the measured pore fluid pressure during the isotropic undrained unloading is reported in Fig. 3. Normalised pore fluid pressure was obtained by dividing the current pore fluid pressure with the correspondent value at the start of unloading, $u_{f0,u}$.

For an initial portion of the unloading stage in Fig. 3, the pore fluid pressure for the gassy samples decreased as much as for the saturated samples. A closer examination of Fig. 2(b) reveals that non-null volumetric strains started being observed only when the cell pressure reached a pressure of about 60% of the initial value (see Table 4). Starting from this point,

Downloaded by [TU Delft Library] on [10/10/18]. Copyright © ICE Publishing, all rights reserved.

Accepted manuscript doi:
10.1680/jgeot.17.P.148

the pore fluid pressure in the gassy samples remained higher than that in the saturated samples.

For all the gassy samples, the pore fluid pressure corresponding to the onset of gas exsolution, reported in Table 4, was below the initial gas-liquid saturation pressure, $u_{l/g,0}$ = 380 kPa, at which the carbonated water solution had been prepared. The main reason for this discrepancy can be ascribed to the different temperatures at which the water was saturated with gas (22° C) and the temperature of the room where the triaxial tests were run (13° C). According to Henry's law, the gas solute mole fraction, χ, in the aqueous phase is proportional to the absolute gas pressure, u_g, through Henry's coefficient H^{xp} (Pa^{-1})

$$H^{xp} = \frac{\chi}{u_g} \tag{3}$$

The dependence of Henry's coefficient on temperature is taken into account with Van't Hoff's equation (Atkins & De Paula, 2014; Sander, 2015):

$$H^{xp}(T) = \frac{M_{H_2O}}{\rho_{H_2O}} H^{cp*} \exp\left(\frac{-\Delta_{sol}H}{R}\left(\frac{1}{T} - \frac{1}{T^*}\right)\right) \tag{4}$$

where H^{cp*} is the concentration Henry's coefficient at the reference temperature (T^*= 298.15 K), equal to 3.3×10^{-4} mol/(m^3Pa), M_{H_2O} is the molar mass of water and ρ_{H_2O} is its temperature dependent density. The term $\Delta_{sol}H$ is referred to as enthalpy of dissolution (Atkins & De Paula, 2014) and depends on the gas species, while R is the gas constant. The solubility in water of N_2, dry air and CO_2 are reported in Table 5 for the temperatures of interest, namely 22 °C and 13 °C.

The dependence of CO_2 Henry's coefficient on temperature gives that the dissolved concentration at 22 °C and relative pressure of 380 kPa corresponds to a relative liquid-gas saturation pressure $u_{l/g,13°}$ = 271 kPa at 13 °C, at which the triaxial tests were performed.

Downloaded by [TU Delft Library] on [10/10/18]. Copyright © ICE Publishing, all rights reserved.

Accepted manuscript doi:
10.1680/jgeot.17.P.148

This change in the liquid-gas saturation pressure may account for most of the difference between the pressure at which the gas was dissolved into the water and the pressure at which it started exsolving during the undrained unloading. Similar delay in gas exsolution was also observed on a soft marine clay (Sultan et al., 2012), although no difference in temperature was reported. Further influence on the gas exsolution pressure might have come from the presence of a small amount of air during the saturation of water with CO_2, which reduced the dissolved CO_2 fraction (Mori et al., 1977), or from the change in the pH of water when flushed into the organic soil material (Appelo & Postma, 2005).

Undrained shearing stage

The results of the shearing stage performed under undrained conditions are reported in terms of stress path in Fig. 4(a), and excess pore fluid pressure, Δu_f in Fig. 4(b). The symbols in the plots correspond to axial strain increments of 2%. Test 1 and Test 6 have an initial overconsolidation ratio, OCR, equal to 1.3 and 2.2, defined as

$$\mathrm{OCR} = \frac{p''_{max}}{p''_{0,s}} \tag{5}$$

where p''_{max} is the maximum mean operative stress applied to the sample during the loading history and $p''_{0,s}$ is the mean operative stress at the start of shear.

As expected, the presence of free gas in the samples increases the pore fluid compressibility upon axial compression, promoting lower excess pore fluid pressure in comparison with fully saturated samples (Fig. 4(b)) and non-null volumetric strain despite the external undrained conditions. The initial vertical traits in the stress paths in Fig. 4(a) of the gassy samples resemble an initial elastic path. With further compression and dissolution of the free gas, the pore pressure rate increases, until the stress paths eventually become parallel to those of the saturated samples. Negligible consequences seem to be caused by the presence of gas on the

Downloaded by [TU Delft Library] on [10/10/18]. Copyright © ICE Publishing, all rights reserved.

Accepted manuscript doi:
10.1680/jgeot.17.P.148

ultimate shear strength of the peat, which occurred with a diffuse failure mode for all the samples, at an axial strain around 0.3.

FABRIC EVIDENCE

To support the interpretation of the experimental results, a fabric investigation was performed, including Micro-CT scans and polarisation microscope micrographs. Two CT-scans were performed on the same sample, the first one in the natural undisturbed state and the second one after gas exsolution. The comparison reported in Fig. 5 reveals that gas exsolution results in the formation of new pores, with characteristic size of 1-2 mm, which are generated by gas expansion in undrained conditions. These are represented by the black spots in the micrographs, while denser elements have brighter appearance. Similar gas bubble radii were observed by den Haan & Kruse (2007), Kettridge & Binley (2008), and Rezanezhad et al. (2010).

Due the low difference between the density of solids and that of the surrounding pore fluid, micro-CT scans do not allow to visualise in detail the fabric of wet peat, which could be revealed only after significant drying. To overcome this limitation and identify relevant fabric features of the wet peat, a companion sample was observed with a polarisation microscope equipped with a digital microscope camera. The peat fabric in Fig. 6 appears to be organised in organic peds, made of organic components such as leaves, roots and stems, and some inorganic particles such as sand grains (white spots in Fig. 5 and Fig. 6). Fibres having different orientation and curvature crossing the organic peds are also evident in Fig. 6. The visible pores in Fig. 6 have a typical size in the range 0.1 - 2 mm, and they can be ascribed to the inter-particle (inter-peds) peat macro-porosity, which dominates the pore fluid response (Rezanezhad et al., 2016).

Downloaded by [TU Delft Library] on [10/10/18]. Copyright © ICE Publishing, all rights reserved.

Accepted manuscript doi:
10.1680/jgeot.17.P.148

DISCUSSION

Pore fluid response during gas exsolution

There is clear evidence that the pore pressure evolution in a gassy soil depends both on the gas-liquid equilibrium and on the mechanical response of the soil skeleton, due to the coupled response being dominated by the relative stiffness of the pore fluid and the soil skeleton. A description of the gas exsolution process is provided by analysing the time evolution of the cell pressure, σ_c, and pore fluid pressure, u_f, reported in Fig. 7(a), Fig. 8(a) and Fig. 9(a). The corresponding time dependent mean operative stress and degree of saturation are displayed in the parallel series of figures (b). A sequence of three stages can be clearly identified, namely:

- stage 1 $\dot{u}_f \cong \dot{\sigma}_c$, $\dot{p}'' \cong 0$ and $\dot{S}r \cong 0$
- stage 2 $\dot{u}_f \ll \dot{\sigma}_c$, $\dot{p}'' \ll 0$ and $\dot{S}r < 0$
- stage 3 $\dot{u}_f \cong \dot{\sigma}_c$, $\dot{p}'' \cong 0$ and $\dot{S}r \ll 0$.

During stage 1, the measured pore fluid pressure decreases commensurately with the cell pressure, almost no gas exsolution takes place, and the mean operative stress keeps nearly constant.

Gas exsolution starts when the pore fluid pressure reaches values in the range 245-210 kPa, depending on the test (see Table 4), which increases the compressibility of the pore fluid. As a result, the total stress reduction is mainly transferred onto the soil skeleton, with a relevant decrease in the mean operative stress. In the final stage 3, the mean operative stress shows very small variation and keeps close to zero (Fig. 7(b), Fig. 8(b) and Fig. 9(b)). The compressibility of the soil skeleton is largely increased and significant gas exsolution and expansion occur.

The corresponding change in the ratio between the compressibility of the pore fluid and that of the soil skeleton is reflected in Fig. 10 in terms of pore pressure parameter B (Skempton,

Downloaded by [TU Delft Library] on [10/10/18]. Copyright © ICE Publishing, all rights reserved.

Accepted manuscript doi:
10.1680/jgeot.17.P.148

1954) for the case of Test 5 and Test 6. During stage 1, the parameter B remains close to 1, as for the case of fully saturated sample. After the onset of the gas exsolution and expansion, during stage 2, the compressibility of the pore fluid increases and the B value decreases. The pore pressure parameter B starts increasing again, when a significant reduction in the mean operative stress occurs, which increases the compressibility of the soil skeleton.

Confining effects on gas exsolution and expansion

A description of the relative volume occupied by the gas bubbles within the porous space can be attempted making reference to the characteristics of the peat fabric visualised in Fig. 5 and Fig. 6, and using the simple schemes in Fig. 11. The sketched porous structure refers to the scale of the interparticles voids, where carbonated water replaced the natural water. For the sake of clarity, only the data from Test 6 are plotted. At the onset of gas exsolution, the bubbles can start growing in the pore space without interacting with the organic peds (i.e. isolated gas bubbles, sub-stage 2A in Fig. 11). As long as the gas bubbles remain confined in the pore space, the response is typically that of a porous medium saturated with a compressible pore fluid. Over further unloading, the gas bubbles expand and coalesce, and they start interacting with the surrounding soil skeleton. The gas pressure starts acting directly on the organic peds in localized contact zones (sub-stage 2B in Fig. 11), and full three phases interaction takes place between organic peds, pore fluid and gas bubbles (Wheeler, 1988b). Pores enlargement occurs, eventually reducing the contact forces between the soil particles. The transition between these two sub-stages occurs with a remarkable decrease in the mean operative stress, which is highlighted by a dramatic increase in the ratio $\Delta p''/\Delta\sigma_c$. With a progressive reduction in the confining stress, gas exsolution and expansion bring to a rearrangement of the soil fabric (stage 3 in Fig. 11), with gas bubbles locally

Downloaded by [TU Delft Library] on [10/10/18]. Copyright © ICE Publishing, all rights reserved.

Accepted manuscript doi:
10.1680/jgeot.17.P.148

interconnected in form of preferential cluster structures, as shown by Kettridge & Binley (2008) and by Rezanezhad et al. (2010) on different peat samples.

The dependence of the volumetric strains on the confining stress can be appreciated with reference to Fig. 12, where the results of all the tests on gassy samples are reported as a function of the current mean operative stress normalised with the value recorded at the beginning of unloading, $p''_{0,u}$. Over stage 2, the volumetric strains are almost linearly dependent on the logarithm of the mean operative stress. At the end of this stage, the recorded volumetric strains range between 4% - 6% for a relatively high change in the operative stress. The majority of free gas is generated only during stage 3, under nearly constant mean operative stress, when previous gas exsolution and expansion have softened the soil fabric. Possible local softening of the soil fabric was suggested during these tests by the observation of gas pockets developing at the boundaries of the samples during the last part of unloading. These were interpreted as the result of local expansion, which allowed preferential gas flow paths towards the external part of the samples (Jommi et al., 2017).

Deviatoric behaviour

The deviatoric response of fibrous peats is dominated by the fibres network. It is generally accepted that in a standard undrained triaxial tests the fibres tend to align horizontally, and provide an internal additional confinement to the sample, which is responsible for very high ultimate strength. The stress-strain curves for the saturated samples (Fig. 13(a)) show continuously increasing deviator stress in the strain range investigated, as typically found on fibrous peats (e.g. Oikawa & Miyakawa, 1980; Cola & Cortellazzo, 2005; Hendry et al., 2012). This feature complicates the definition of a failure criterion for the investigated material, because an asymptotic value for the deviator stress is not found, and the stress path approaches the Tension Cut Off (TCO) line (Fig. 4(a)). Among different possible choices, in

Downloaded by [TU Delft Library] on [10/10/18]. Copyright © ICE Publishing, all rights reserved.

Accepted manuscript doi:
10.1680/jgeot.17.P.148

this study failure is assumed to be triggered in correspondence of the start of the linear hardening portion of the q-ε_a stress-strain curve (Kanmuri et al., 1998). The rationale behind this choice is that this criterion corresponds to the transition between contractive and dilatant behaviour, which identifies the critical state for the peat matrix if the radial stretching effect of fibres is neglected. The transition between contractive and dilatant behaviour during an undrained deviatoric compression stage occurs when the pore pressure parameter $a = -\Delta p''/\Delta q$ becomes zero, passing from positive to negative values (contractive behaviour is characterised by $a > 0$ while dilatant response by $a < 0$, see Wood, 1990). It is worth noting that this criterion was proposed for fibrous peats by Oikawa & Miyakawa (1980) and adopted by Mesri & Ajlouni (2007). The mechanical ground of this criterion had been discussed for dense sands in undrained compression by Nova (1977), who demonstrated that stress ratios higher than the critical stress ratio M can be reached after $a = 0$ is overpassed due to dilation in the hardening regime.

The evolution of the pore pressure parameter a for the saturated samples (Test 1 and Test 2) is reported in Fig. 13(b). The transition from contractive to dilatant behaviour of the saturated samples occurred for axial strains of 7% and 12%, in Test 1 and Test 2 respectively, for an average stress ratio $\eta = 2.3$. The evolution of the measured fluid pressure for the gassy samples is reported in Fig.14. Significant higher axial strains, in the range 16% - 20%, needed to be applied to the gassy samples in order to switch from contractive to dilatant behaviour. As this transition is associated to the start of significant confinement effect offered by the fibres, it can be concluded that the dominant effect of gas on the deviatoric behaviour is to delay the fibres stretch significantly.

To provide further insight into the deformation mechanism and to appreciate this delay in the fibres stretch contribution, the operative axial stress is reported in Fig. 15(a) for the normally

Downloaded by [TU Delft Library] on [10/10/18]. Copyright © ICE Publishing, all rights reserved.

Accepted manuscript doi:
10.1680/jgeot.17.P.148

consolidated saturated sample and in Fig. 15(b) for the gassy samples. The results are normalised for each test with the operative axial stress at the start of shearing, $\sigma''_{a0,s}$. The fully saturated sample presents the typical response of saturated peats, with the operative axial stress increasing steadily with the axial strain. However, for gassy samples there is a significant intermediate portion of the response with almost constant operative axial stress, despite the increasing axial strain. The extension of this trait increases with the initial gas fraction previously exsolved, suggesting that significant rearrangement of the peat fabric must occur before stretching of the fibres starts being effective in contributing to the mobilised strength. Starting from the fabric evidence in Fig. 6 and the sketch in Fig. 11, it can be inferred that gas expansion causing an enlargement of the pores will be accompanied by distortion and bending of the fibres (Stage 3 in Fig. 11). This effect needs to be compensated by high strains during deviatoric compression before the fibres start stretching.

Eventually, the stress ratio corresponding to the onset of failure, detected by the condition $a = \Delta p'' = 0$, is similar for the saturated and the gassy samples (Fig. 16). Slightly higher values can be reached by gassy samples at the expenses of much higher axial strains, which increase with the volumetric gas fraction at the beginning of shear.

These results show that the shear strength of the tested peat is hardly affected by the presence of gas, or even slightly increased if the criterion $a = \Delta p'' = 0$ is adopted to discriminate the onset of failure. However, the delay in mobilised shear strength due to gas compression and fibres stretching results in a dramatic effect on serviceability and ultimate limit states criteria based on mobilised shear strength at given axial strain thresholds. To quantify this remark, Fig. 17 reports the mobilised friction angle, φ'_m, of the saturated and gassy samples in correspondence of typical reference axial strains of 2% and 5%, often used in traditional assessment approaches. On average, a reduction of 30% - 40% in the mobilised friction angle

Downloaded by [TU Delft Library] on [10/10/18]. Copyright © ICE Publishing, all rights reserved.

Accepted manuscript doi:
10.1680/jgeot.17.P.148

of gassy samples compared to saturated samples is observed at both axial strains of 2% and 5%.

SUMMARY AND CONCLUSIONS

Biodegradation of peat generates gases in the soil water, which can exsolve when the equilibrium pressure decreases due to changes in stress, temperature or water pressure. The potential consequences of these gases on the mechanical behaviour of peats have been systematically investigated by means of a series of triaxial tests on natural peat samples from Katwoude in the Netherlands. Controlled amounts of gas were generated by unloading the samples under undrained conditions, after flushing them with carbonated water. A gas fraction in the range 4% to 16% was generated, which replicates the typical amount of gas found in peat layers in the field.

The volumetric and the deviatoric stress-strain responses, as well as the strength have been investigated. During isotropic unloading, gas exsolution and expansion is ruled by the relative stiffness of the pore fluid over that of the solid skeleton. With respect to other gassy soils investigated in the past, the very high compressibility of peats decreases the rate of gas exsolution. Most of gas expansion takes place at very low stress, when the fabric can be locally softened, allowing for gas coalescence and migration. The mechanical response upon undrained unloading is characterised by gas-soil matrix interaction phenomena. As long as the gas bubbles remain confined in the pores space, the typical response of a porous medium saturated with a compressible pore fluid is observed. However, with further gas exsolution and expansion, gas bubbles start acting directly on the soil skeleton. The contact forces between the organic peds are reduced, which rapidly decreases the operative mean stress. Pore enlargement and significant soil matrix changes are expected to occur, until the gas

Downloaded by [TU Delft Library] on [10/10/18]. Copyright © ICE Publishing, all rights reserved.

Accepted manuscript doi:
10.1680/jgeot.17.P.148

bubbles become locally interconnected in gas cluster and the soil matrix is not able to contrast further gas expansion.

Volumetric strains due to gas compression and dissolution during shearing occur for gassy samples, despite the external undrained conditions. Both fully saturated and gassy samples showed diffuse failure mode. The stress ratio at the onset of failure, defined as the transition from contractive to dilatant response, is not significantly affected by the presence of the gas fraction. However, the pre-failure stress-strain relationship for gassy samples is remarkably different from that of fully saturated specimens, with a dramatic reduction in the mobilised shear strength and mobilised friction angle for given axial strain levels. The volumetric strains experienced by the soil matrix delay the peat fibres stretching, and their contribution to shear strength.

The experimental study has been started to evaluate whether and how the presence of gas should be accounted for in the safety assessment of earth structures founded on peat, which are subjected to loading-unloading and thermal cycles, as well as changes in the atmospheric conditions, during their service life. The results suggest that the presence of gas should be carefully considered in the assessment of serviceability limit states. When total stress or pore pressure are reduced, for example due to excavation or dewatering, gas exsolution and expansion will occur, decreasing the operative stress and eventually increasing the soil skeleton compressibility. The effects appear to become dramatic at low total stresses, which is often the case for peat foundation layers at the toe of embankments.

The presence of gas becomes also extremely relevant when ultimate limit states are assessed by choosing an operative shear strength defined on strain thresholds. The compressibility of the gas phase and the delayed stretching of fibres largely reduce the mobilised friction angle for comparable strain thresholds.

Downloaded by [TU Delft Library] on [10/10/18]. Copyright © ICE Publishing, all rights reserved.

Accepted manuscript doi:
10.1680/jgeot.17.P.148

ACKNOWLEDGMENTS

The first two authors gratefully acknowledge the financial support of Deltares through the project "Gasvorming", in the framework of the wider investigation "Dijken op Veen II" financed by Rijkswaterstaat, NL. The third author acknowledges the scholarship awarded from Politecnico di Milano, which supported his stay at Delft University of Technology.

LIST OF SYMBOLS

N	loss of ignition	[-]
OC	organic content	[-]
γ	unit weight	[kN/m^3]
Gs	specific gravity	[-]
n_0	initial porosity	[-]
e_0	initial void ratio	[-]
w_0	initial water content	[-]
Sr	degree of saturation	[-]
T	temperature	[K]
T^*	reference temperature 298.15 K	[K]
RH	relative humidity	[-]
$u_{l/g,0}$	initial gas-liquid saturation pressure	[kPa]
$u_{l/g,13^\circ}$	gas-liquid saturation pressure at 13 °C	[kPa]
u_g	absolute gas pressure	[kPa]
χ	gas solute mole fraction	[-]
H^{cp}	Henry's coefficient of solubility (via concentration)	[mol/(m^{3}Pa)]
H^{cp*}	Henry's coefficient of solubility at T^* (via concentration)	[mol/(m^{3}Pa)]

Downloaded by [TU Delft Library] on [10/10/18]. Copyright © ICE Publishing, all rights reserved.

Accepted manuscript doi:
10.1680/jgeot.17.P.148

H^{xp}	Henry's coefficient of solubility (via mole fraction)	[1/Pa]
ρ_{H_2O}	density of water	[kg/m^3]
M_{H_2O}	molar mass of water	[kg/mol]
$\Delta_{sol}H$	enthalpy of dissolution	[J/mol]
R	gas constant	[J/(mol K)]
σ_c	cell pressure	[kPa]
$\sigma_{c0,u}$	cell pressure at the beginning of unloading	[kPa]
$\Delta\sigma_c$	cell pressure increment	[kPa]
p	total mean stress	[kPa]
u_b	back pressure	[kPa]
u_f	pore fluid pressure	[kPa]
$u_{f0,u}$	pore fluid pressure at the beginning of unloading	[kPa]
Δu_f	excess pore fluid pressure during shear	[kPa]
p''	mean operative stress	[kPa]
p''_{max}	maximum mean operative stress pre-shear	[kPa]
$p''_{0,u}$	mean operative stress at the beginning of unloading	[kPa]
$p''_{0,s}$	mean operative stress at the beginning of shear	[kPa]
OCR	overconsolidation ratio	[-]
σ''_a	operative axial stress	[kPa]
σ''_r	operative radial stress	[kPa]
$\sigma''_{a0,s}$	operative axial stress at the beginning of shear	[kPa]
q	deviatoric stress	[kPa]
η	stress ratio	[-]

Downloaded by [TU Delft Library] on [10/10/18]. Copyright © ICE Publishing, all rights reserved.

Accepted manuscript doi:
10.1680/jgeot.17.P.148

ε_a	axial strain	[-]
ε_p	volumetric strain	[-]
$\dot{\sigma}_c$	rate of cell pressure change	[kPa/h]
$\dot{u}_f$	rate of pore fluid pressure change	[kPa/h]
$\dot{p}''$	rate of mean operative stress change	[kPa/h]
$\dot{S}_r$	rate of degree of saturation change	[-/h]
a	pore pressure parameter	[-]
B	pore pressure parameter	[-]
$\Delta p''$	mean operative stress increment	[kPa]
Δq	deviatoric stress increment	[kPa]
M	critical stress ratio	[-]
φ'_m	mobilised friction angle	[°]

Downloaded by [TU Delft Library] on [10/10/18]. Copyright © ICE Publishing, all rights reserved.

Accepted manuscript doi:
10.1680/jgeot.17.P.148

References

Acharya, M. P., Hendry, M. T. & Martin, C. D. (2016a). Effect of gas bubbles on pore pressure response in peat beneath a railway embankment. *Can. Geotech. J.* 53, No. 5, 765-772.

Acharya, M. P., Hendry, M. T. & Martin, C. D. (2016b). Thermally induced pore pressure response in peat beneath a railway embankment. *International Journal of Geotechnical Engineering* 10, No. 2, 145-154.

Amaratunga, A. & Grozic, J. L. H. (2009). On the undrained unloading behaviour of gassy sands. *Can. Geotech. J.* 46, No. 11, 1267-1276.

Appelo, C. A. J. & Postma, D. (2005). Geochemistry, groundwater and pollution, 2nd edn. Leiden: Balkema.

ASTM (2014a). ASTM D5550–14: Standard test method for specific gravity of soil solids by gas pycnometer. West Conshohocken, PA, USA: ASTM International.

ASTM (2014b). ASTM D2974-14: Standard test methods for moisture, ash, and organic matter of peat and other organic soils. West Conshohocken, PA, USA: ASTM International.

Atkins, P. W. & De Paula, J. (2014). Physical Chemistry: Thermodynamics, Structure, and Change. Oxford University Press.

Baird, A. J. & Waldron, S. (2003). Shallow horizontal groundwater flow in peatlands is reduced by bacteriogenic gas production. *Geophys. Res. Lett.* 30, No. 20, 1-4.

Beckwith, C. W. & Baird, A. J. (2001). Effect of biogenic gas bubbles on water flow through poorly decomposed blanket peat. *Water Resour. Res.* 37, No. 3, 551– 558.

Brown, A., Mathur, S. P. & Kushner, D. J. (1989). An ombrotrophic bog as a methane reservoir. *Global Biogeochem. Cycles* 3, No.3, 205–213 .

Downloaded by [TU Delft Library] on [10/10/18]. Copyright © ICE Publishing, all rights reserved.

Accepted manuscript doi:
10.1680/jgeot.17.P.148

Buttler, A. J., Dinel, H., Lévesque, M., & Mathur, S. P. (1991). The relation between movement of subsurface water and gaseous methane in a basin bog with a novel instrument. *Can. J. Soil Sci.* 71, No. 4, 427–438.

Cola, S. & Cortellazzo, G. (2005). The shear strength behavior of two peaty soils. *Geotechnical & Geological Engineering* 23, No. 6, 679–695.

Den Haan, E. J. & Kruse, G. A. M. (2007). Characterisation and engineering properties of Dutch peats. In *Proceedings of the Second International Workshop on Characterisation and Engineering Properties of Natural Soils*, (eds. Phoon, Hight, Leroueil & Tan), Singapore, 2101-2133.

De Vries, G. & De Bruijn, H. T. J. (2014). Dijken op Veen II Factual report laboratorium- en grondonderzoek. Internal report, Deltares.

Dinel, H., Mathur, S. P., Brown, A. & Lévesque, M. (1988). A field study of the effect of depth on methane production in peatland waters: equipment and preliminary results. *Journal of Ecology* 76, No. 4, 1083– 1091.

Gens, A. (1996). Constitutive modelling: Application to compacted soils. In *Proc. 1st Int. Conf. On Unsaturated Soils*, Balkema, Rotterdam, 3, 1179-1200.

Glaser, P. H., Chanton, J. P., Morin, P., Rosenberry, D. O., Siegel, D. I., Ruud, O., Chasar, L. I. & Reeve, A. S. (2004). Surface deformations as indicators of deep ebullition fluxes in a large northern peatland. *Global Biogeochem. Cycles* 18, No. 1, 1-15.

Grozic, J. L., Robertson, P. K., & Morgenstern, N. R. (1999). The behavior of loose gassy sand. *Can. Geotech. J.* 36, No. 3, 482-492.

Grozic, J. L., Robertson, P. K., & Morgenstern, N. R. (2000). Cyclic liquefaction of loose gassy sand. *Can. Geotech. J.* 37, No. 4, 843-856.

Downloaded by [TU Delft Library] on [10/10/18]. Copyright © ICE Publishing, all rights reserved.

Accepted manuscript doi:
10.1680/jgeot.17.P.148

Grozic, J. L. H., Nadim, F., & Kvalstad, T. J. (2005). On the undrained shear strength of gassy clays. *Computers and Geotechnics* 32, No. 7, 483-490.

Head, K. H. (2014). Manual of soil laboratory testing – Vol. I: Soil classification and compaction tests, 3rd edn. Dunbeath, UK: Whitteles Publishing.

Hendry, M. T., Sharma, J. S., Martin, C. D. & Barbour, S. L. (2012). Effect of fibre content and structure on anisotropic elastic stiffness and shear strength of peats. *Can. Geotech. J.* 49, No. 4, 403–415.

Hight, D. W. & Leroueil, S. (2003). Characterisation of soils for engineering purposes. In *Characterisation and engineering properties of natural soils* (eds T. S Tan, K. K. Phoon, D. W. Hight and S. Leroueil), 255–362. Lisse, the Netherlands: Balkema.

Jommi, C. (2000). Remarks on the constitutive modelling of unsaturated soils. In *Experimental Evidence and Theoretical Approaches in Unsaturated Soils*, (eds. Tarantino & Mancuso) Balkema, Rotterdam, 139-153.

Jommi, C., Muraro, S., Trivellato, E. & Zwanenburg, C. (2017). Evidences of the effects of free gas on the hydro-mechanical behaviour of peat. In *Advances in Laboratory Testing and Modelling of Soils and Shales*, Springer, Cham., 112-119.

Kanmuri, H., Kato, M., Suzuki, O. & Hirose, E. (1998). Shear strength of K0 consolidated undisturbed peat. In *Problematic Soils*, (eds. Yanagisawa, Moroto & Mitachi), Rotterdam, the Netherlands: Balkema, 25-28.

Kellner, E., Price, J. S. & Waddington, J. M. (2004). Pressure variations in peat as a result of gas bubble dynamics. *Hydrol. Processes* 18, No. 13, 2599– 2605.

Kellner, E., Waddington, J. M. & Price, J. S. (2005). Dynamics of biogenic gas bubbles in peat: Potential effects on water storage and peat deformation. *Water Resources Research* 41, No. 8, 1-12.

Downloaded by [TU Delft Library] on [10/10/18]. Copyright © ICE Publishing, all rights reserved.

Accepted manuscript doi:
10.1680/jgeot.17.P.148

Kettridge, N. & Binley, A. (2008). X-ray computed tomography of peat soils: measuring gas content and peat structure. *Hydrological Processes* 22, No. 25, 4827–4837.

Landva, A. O. & Pheeney, P. E. (1980). Peat fabric and structure. *Can. Geotech. J.* 17, No. 3, 416-435.

Lunne, T., Berre, T., Stranvik, S., Andersen, K. H. & Tjelta, T. I. (2001). Deepwater sample disturbance due to stress relief. In *Proceedings of the OTRC 2001 international conference*, Houston, TX, 64–85.

Mori, Y., Hijikata, K., & Nagatani, T. (1977). Fundamental study of bubble dissolution in liquid. *International Journal of Heat and Mass Transfer* 20, No. 1, 41-50.

Mesri, G., & Ajlouni, M. (2007). Engineering properties of fibrous peats. *Journal of Geotechnical and Geoenvironmental Engineering*, 133, No. 7, 850-866.

Nageswaran, S. (1983). Effect of gas bubbles on the sea-bed behavior. PhD thesis, Oxford University, Oxford, England.

Nova R. (1977). On the hardening of soils. *Archiwum Mechaniki Stosowanej*, 29, 445–458.

Oikawa, H. & Miyakawa, I. (1980). Undrained Shear Characteristics of Peat (in Japanese*). Soils and Foundations* 20, No. 3, 91-100.

Rad, N. S., Vianna, A. J. D. & Berre, T. (1994). Gas in Soils. II: Effect of gas on undrained static and cyclic strength of sand. *Journal of Geotechnical Engineering* 120, No. 4, 716-736.

Reynolds, W. D., Brown, D. A., Mathur, S. P. & Overend, R. P. (1992). Effect of in-situ gas accumulation on the hydraulic conductivity of peat. *Soil Science* 153, No. 5, 397–408.

Rezanezhad, F., Quinton,W. L., Price, J. S., Elliot, T. R., Elrick, D. & Shook, K. R. (2010). Influence of pore size and geometry on peat unsaturated hydraulic conductivity

Downloaded by [TU Delft Library] on [10/10/18]. Copyright © ICE Publishing, all rights reserved.

Accepted manuscript doi:
10.1680/jgeot.17.P.148

computed from 3D computed tomography image analysis. *Hydrol. Process*. 24, No. 21, 2983–2994.

Rezanezhad, F., Price, J. S., Quinton, W. L., Lennartz, B., Milojevic, T., & Van Cappellen, P. (2016). Structure of peat soils and implications for water storage, flow and solute transport: A review update for geochemists. *Chemical Geology* 429, 75-84.

Rosenberry, D. O., Glaser, P. H., Siegel, D. I. & Weeks, E. P. (2003). Use of hydraulic head to estimate volumetric gas content and ebullition flux in northern peatlands. *Water Resources Research* 39, No. 3, 1-10.

Sander, R. (2015). Compilation of Henry's law constants (version 4.0) for water as solvent. *Atmos. Chem. Phys*.15, 4399-4981.

Sills, G. C., Wheeler, S. J., Thomas, S. D. & Gardner, T. N. (1991). Behaviour of offshore soils containing gas bubbles. *Géotechnique* 41, No. 2, 227-241.

Sills, G. C. & Gonzalez, R. (2001). Consolidation of naturally gassy soft soil. *Géotechnique* 51, No. 7, 629-639.

Skempton, A. W. (1954). The pore-pressure coefficients A and B. *Géotechnique* 4, No. 4, 143-147.

Skempton, A. W. & Petley, D. J. (1970). Ignition loss and other properties of peats and clays from Avonmouth, King's Lynn, and Cranberry Moss. *Géotechnique* 20, No. 4, 343-356.

Sobkowicz, J. C. & Morgenstern, N. R. (1984). The undrained equilibrium behaviour of gassy sediments. *Can. Geotech. J.* 21, No. 3, 439–448.

Strack, M., Kellner, E. & Waddington, J. M. (2005). Dynamics of biogenic gas bubbles in peat and their effects on peatland biogeochemistry. *Global Biogeochemical Cycles* 19, No. 1, 1-9.

Downloaded by [TU Delft Library] on [10/10/18]. Copyright © ICE Publishing, all rights reserved.

Accepted manuscript doi:
10.1680/jgeot.17.P.148

Sultan, N., Gaudin, M., Berne, S., Canals, M., Urgeles, R. & Lafuerza, S. (2007). Analysis of slope failures in submarine canyon heads: an example from the Gulf of Lions. *J. Geophys. Res.* 112, 1-29.

Sultan, N., De Gennaro, V. & Puech, A. (2012). Mechanical behaviour of gas-charged marine plastic sediments. *Géotechnique* 62, No. 9, 751–766.

Tokida, T., Miyazaki, T. & Mizoguchi, M. (2005). Ebullition of methane from peat with falling atmospheric pressure. *Geophysical Research Letters* 32, No. 13, 1-4.

Tokida, T., Miyazaki, T., Mizoguchi, M., Nagata, O., Takakai, F., Kagemoto, A. & Hatano, R. (2007). Falling atmosphere pressure as a trigger for methane ebullition from peatland. *Global Biogeochemical Cycles* 21, No. 2, 1-8.

Van der Putte, E. (2014). An insight in the micro fabric of gassy and unsaturated peat. MSc Thesis, Delft University of Technology.

Vonk, B. F. (1994). Some aspects of the engineering practice regarding peat in small polder dykes. In *Advances in understanding and modelling mechanical behaviour of peat* (eds. Den Haan, Termaat & Edil), Rotterdam, the Netherlands: Balkema, 389–402.

Waddington, J. M., Harrison, K., Kellner, E. & Baird. A. J. (2009). Effect of atmospheric pressure and temperature on entrapped gas content in peat. *Hydrological Processes* 23, No. 20, 2970–2980.

Wheeler, S. J. (1988a). The undrained shear-strength of soils containing large gas-bubbles. *Géotechnique* 38, No. 3, 399–413.

Wheeler, S. J. (1988b). A conceptual model for soils containing large gas bubbles. *Géotechnique* 38, No. 3, 389-397.

Wood, D. M. (1990). Soil behaviour and critical state soil mechanics. *Cambridge university press*.

Downloaded by [TU Delft Library] on [10/10/18]. Copyright © ICE Publishing, all rights reserved.

Accepted manuscript doi:
10.1680/jgeot.17.P.148

Zwanenburg, C. (2013). Dikes on Peat: analysis of field trials. Internal report, Deltares.

LIST OF TABLES

Downloaded by [TU Delft Library] on [10/10/18]. Copyright © ICE Publishing, all rights reserved.

Accepted manuscript doi:
10.1680/jgeot.17.P.148

Table 1. Index properties of the tested specimens

Sample	Depth form the ground level z (m)	Unit weight γ (kN/m^3)	Specific gravity Gs (-)	Porosity n_0 (-)	Void ratio e_0 (-)	Water content w_0 (-)	Degree of saturation Sr (-)
Test 1	1.1-1.3	9.90	1.48	0.91	9.59	6.50	1.00
Test 2	1.1-1.3	10.1	1.47	0.90	9.21	6.20	0.99
Test 3	1.6-1.8	11.0	1.37	0.92	12.04	7.35	0.84
Test 4	1.7-1.9	10.4	1.40	0.91	9.89	6.63	0.94
Test 5	2.3-2.5	10.2	1.45	0.91	10.03	6.38	0.92
Test 6	1.7-1.9	10.4	1.43	0.92	10.78	6.53	0.87

Table 2. Measured stress variables for Test 1 and Test 2 performed on saturated specimens. The values refer to the end of the steps unless otherwise specified

	Test 1 H_2O			Test 2 N_2		
Stage	σ_c	u_b	u_f	σ_c	u_b	u_f
	(kPa)			(kPa)		
Flushing	421	407	411	407	397	398
1st consolidation	420	405	406	426	403	404
Undrained unloading	53	-	38	51	-	30
Start of undrained shear	51	-	38	52	-	31

Downloaded by [TU Delft Library] on [10/10/18]. Copyright © ICE Publishing, all rights reserved.

Accepted manuscript doi:
10.1680/jgeot.17.P.148

Table 3. Measured stress variables for Test 3, 4, 5 and 6 on gassy specimens. The values refer to the end of the steps unless otherwise specified

	Test 3 CO_2			Test 4 CO_2			Test 5 CO_2			Test 6 CO_2		
Stage	σ_c	u_b	u_f	σ_c	u_b	u_f	σ_c	u_b	u_f	σ_c	u_b	u_f
	(kPa)			(kPa)			(kPa)			(kPa)		
Flushing	407	402	404	408	402	403	409	402	403	410	405	406
1st consolidation	404	383	383	406	382	382	408	387	387	409	383	384
Undrained unloading	51	-	49	63	-	58	52	-	50	65	-	64
2nd consolidation	68	50	51	79	55	55	70	50	51	98	-*	87
Start of undrained shear	69	-	50	80	-	53	71	-	48	100	-	88

* For Test 6 CO_2, the 2nd consolidation stage was substituted with a compression at closed drainage

Downloaded by [TU Delft Library] on [10/10/18]. Copyright © ICE Publishing, all rights reserved.

Accepted manuscript doi:
10.1680/jgeot.17.P.148

Table 4. Imposed gas-liquid saturation pressure, cell pressure and pore fluid pressure at the onset of gas exsolution

Test	$u_{l/g,0}$ (kPa)	σ_c (kPa)	u_f (kPa)
Test 3 CO_2	380	250	232
Test 4 CO_2	380	270	247
Test 5 CO_2	380	241	222
Test 6 CO_2	380	235	211

Table 5. Molar solubility of relevant gases at different temperatures

H^{cp}	Temperature	
mol/(m^3Pa)	22 °C	13 °C
N_2	6.7×10^{-6}	7.7×10^{-6}
Air	9.2×10^{-6}	1.1×10^{-5}
CO_2	3.6×10^{-4}	4.6×10^{-4}

Downloaded by [TU Delft Library] on [10/10/18]. Copyright © ICE Publishing, all rights reserved.

Accepted manuscript doi:
10.1680/jgeot.17.P.148

List of Figures

Downloaded by [TU Delft Library] on [10/10/18]. Copyright © ICE Publishing, all rights reserved.

Accepted manuscript doi:
10.1680/jgeot.17.P.148

Downloaded by [TU Delft Library] on [10/10/18]. Copyright © ICE Publishing, all rights reserved.

Accepted manuscript doi:
10.1680/jgeot.17.P.148

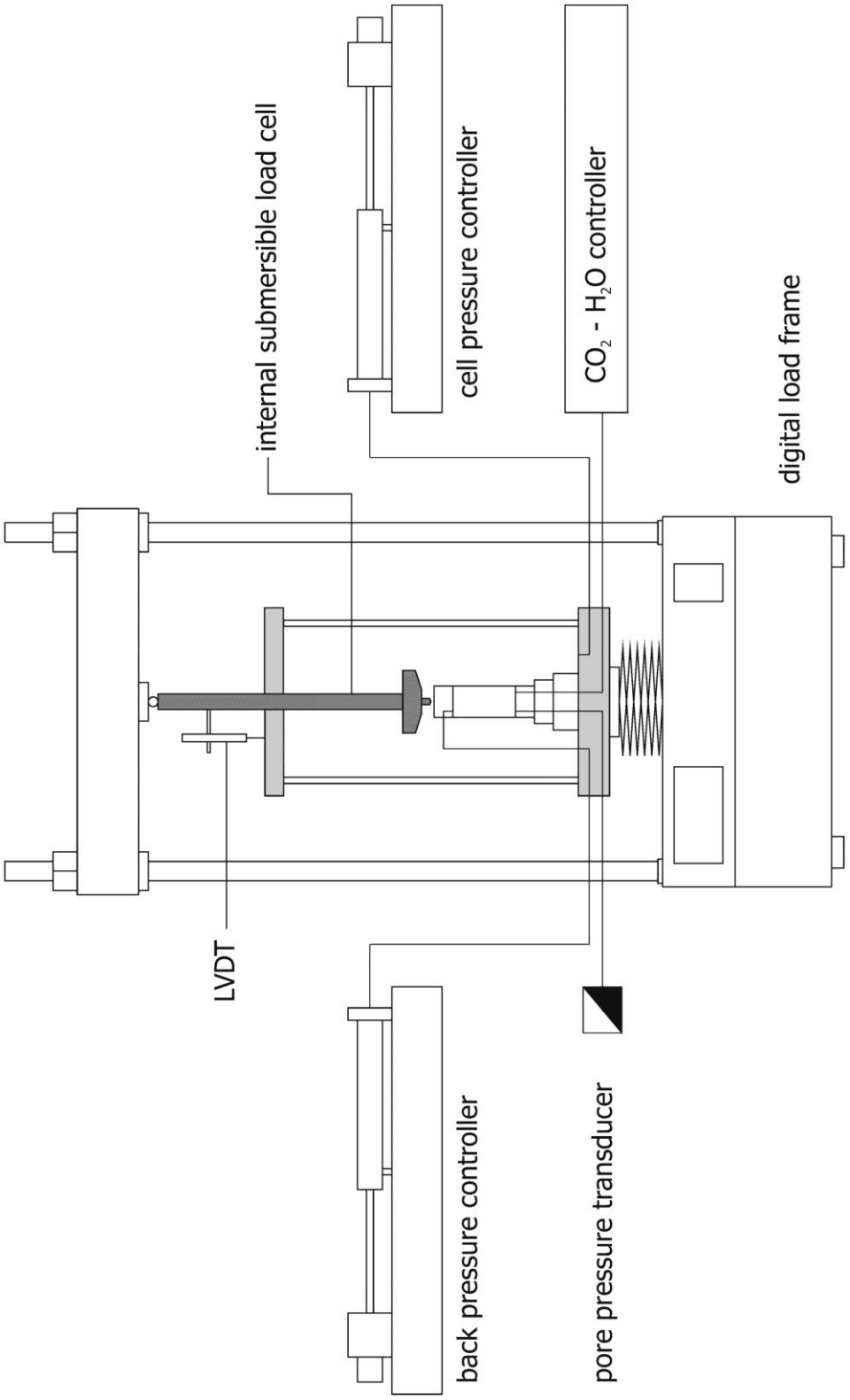

Jommi_Fig_1.jpg

Downloaded by [TU Delft Library] on [10/10/18]. Copyright © ICE Publishing, all rights reserved.

Accepted manuscript doi:
10.1680/jgeot.17.P.148

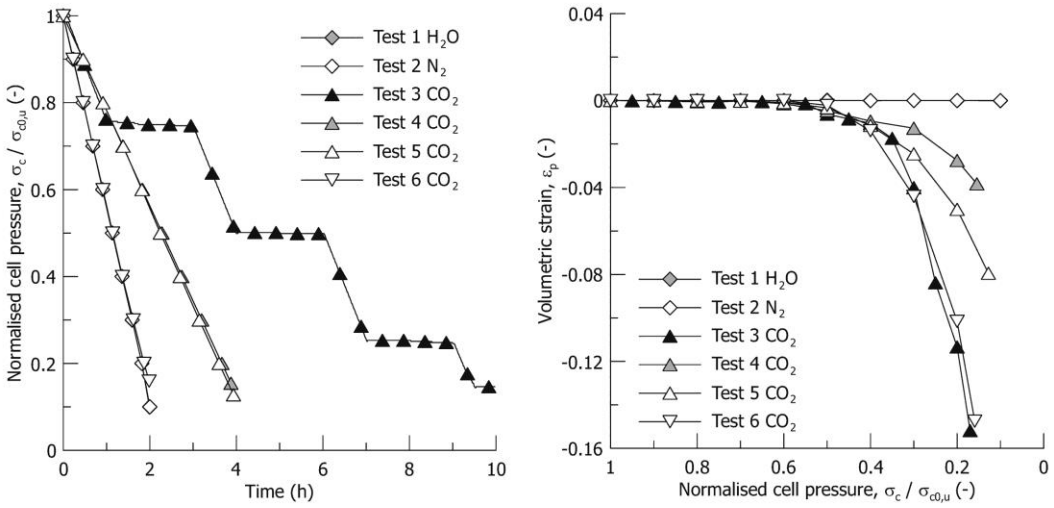

a) b)

Jommi_Fig_2.jpg

Downloaded by [TU Delft Library] on [10/10/18]. Copyright © ICE Publishing, all rights reserved.

Accepted manuscript doi:
10.1680/jgeot.17.P.148

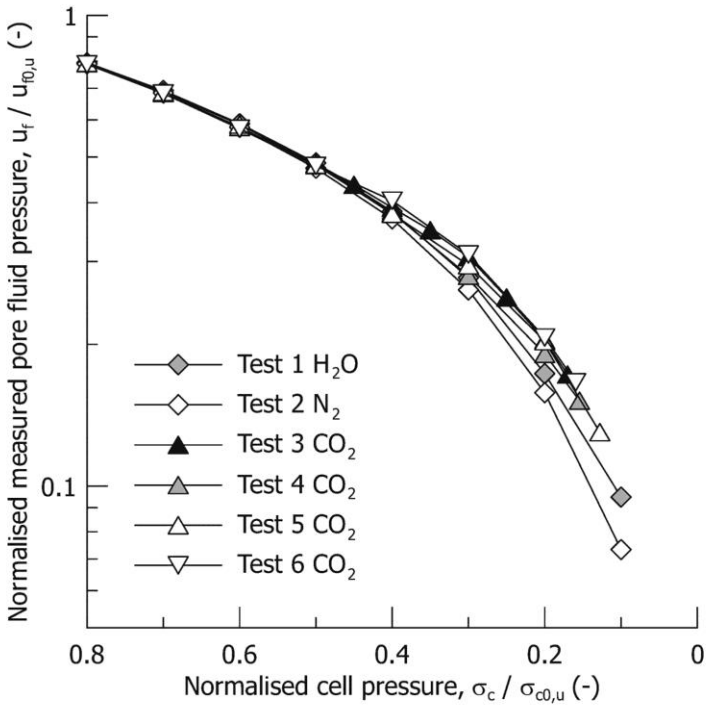

Jommi_Fig_3.jpg

Downloaded by [TU Delft Library] on [10/10/18]. Copyright © ICE Publishing, all rights reserved.

Accepted manuscript doi:
10.1680/jgeot.17.P.148

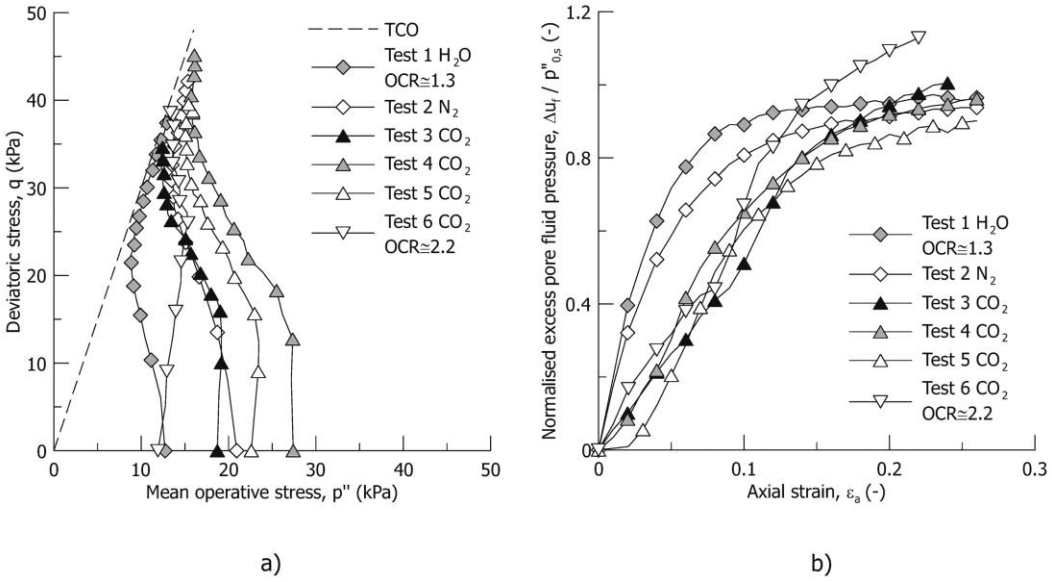

Jommi_Fig_4.jpg

Downloaded by [TU Delft Library] on [10/10/18]. Copyright © ICE Publishing, all rights reserved.

Accepted manuscript doi:
10.1680/jgeot.17.P.148

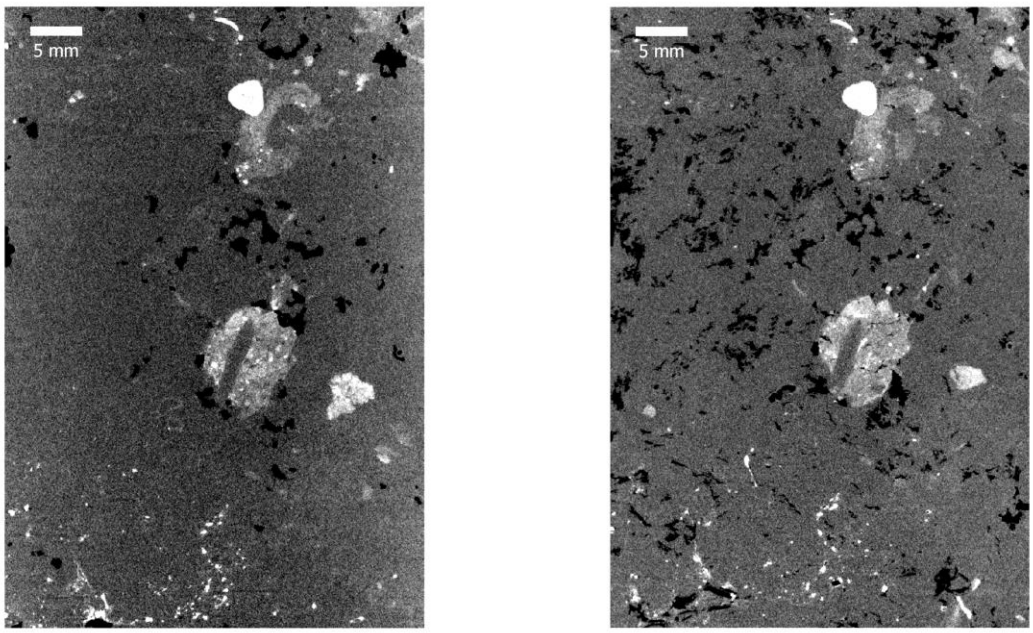

a) b)

Jommi_Fig_5.jpg

Downloaded by [TU Delft Library] on [10/10/18]. Copyright © ICE Publishing, all rights reserved.

Accepted manuscript doi:
10.1680/jgeot.17.P.148

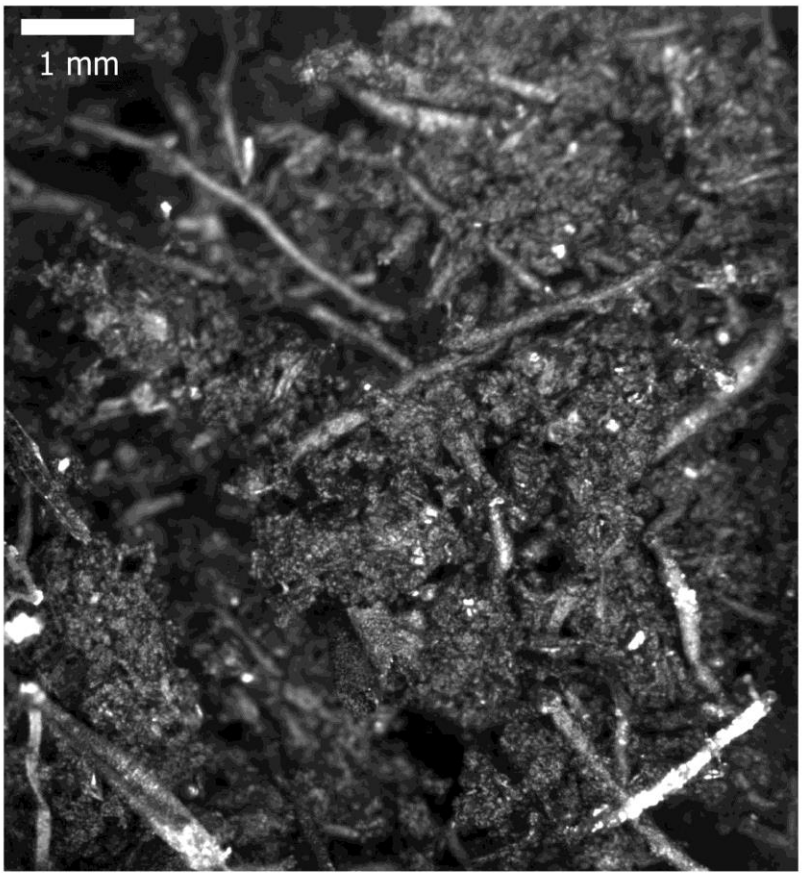

Jommi_Fig_6.jpg

Downloaded by [TU Delft Library] on [10/10/18]. Copyright © ICE Publishing, all rights reserved.

Accepted manuscript doi:
10.1680/jgeot.17.P.148

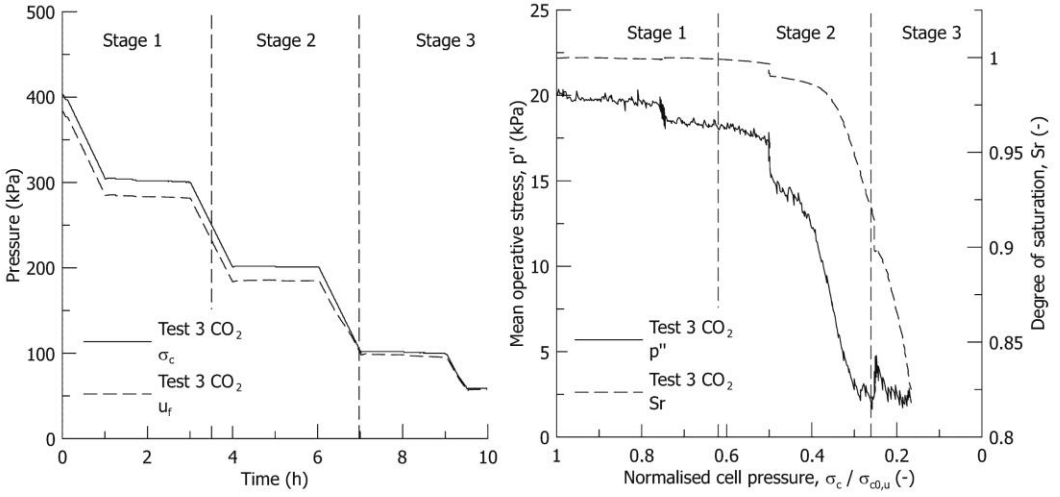

a) b)

Jommi_Fig_7.jpg

Downloaded by [TU Delft Library] on [10/10/18]. Copyright © ICE Publishing, all rights reserved.

Accepted manuscript doi:
10.1680/jgeot.17.P.148

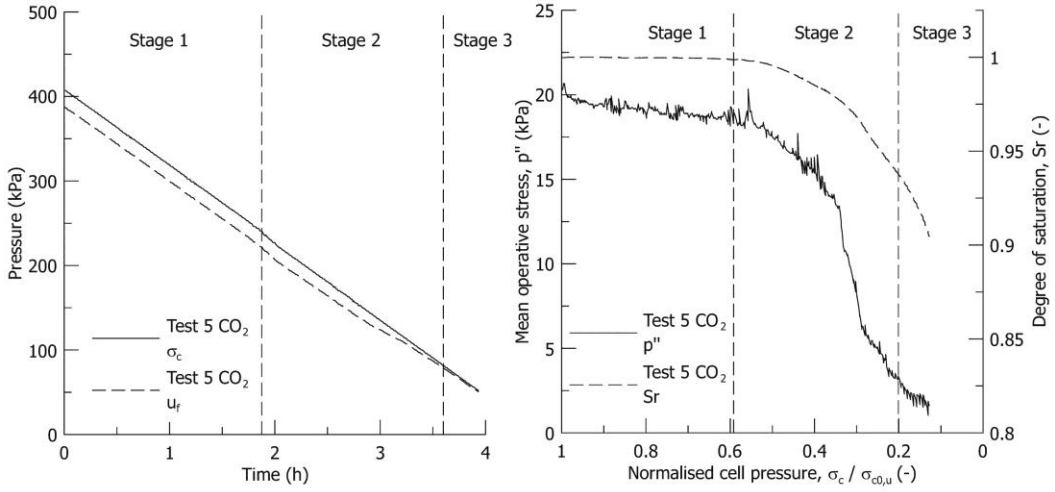

a) b)

Jommi_Fig_8.jpg

Downloaded by [TU Delft Library] on [10/10/18]. Copyright © ICE Publishing, all rights reserved.

Accepted manuscript doi:
10.1680/jgeot.17.P.148

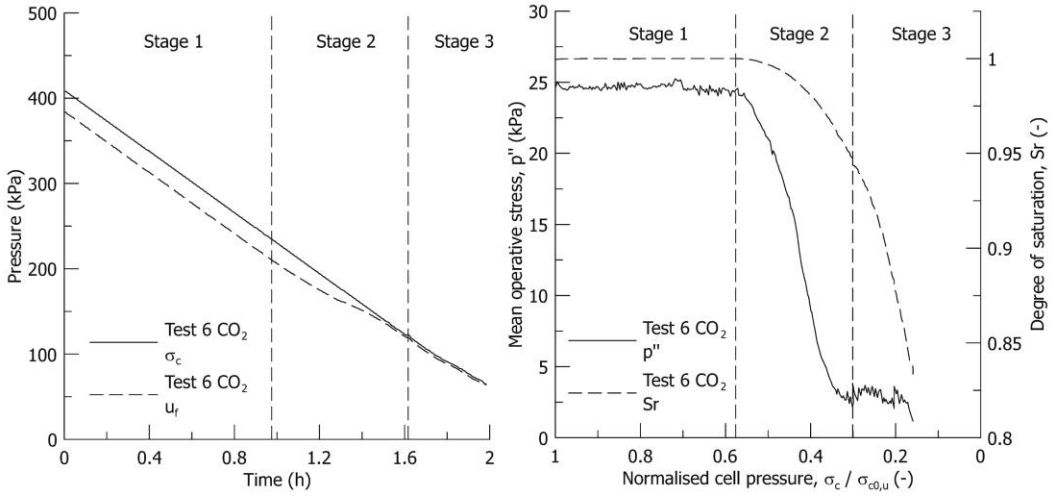

a) b)

Jommi_Fig_9.jpg

Downloaded by [TU Delft Library] on [10/10/18]. Copyright © ICE Publishing, all rights reserved.

Accepted manuscript doi:
10.1680/jgeot.17.P.148

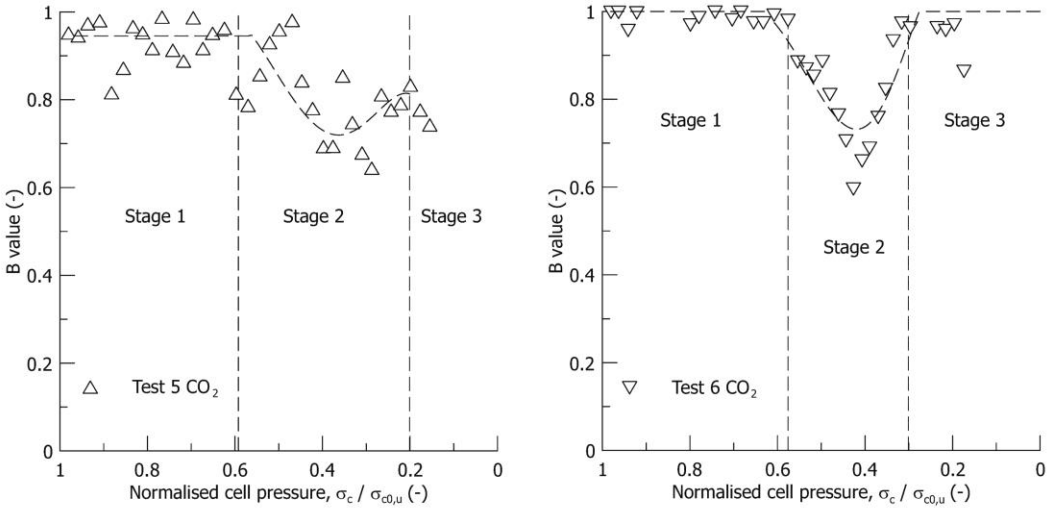

a) b)

Jommi_Fig_10.jpg

Downloaded by [TU Delft Library] on [10/10/18]. Copyright © ICE Publishing, all rights reserved.

Accepted manuscript doi:
10.1680/jgeot.17.P.148

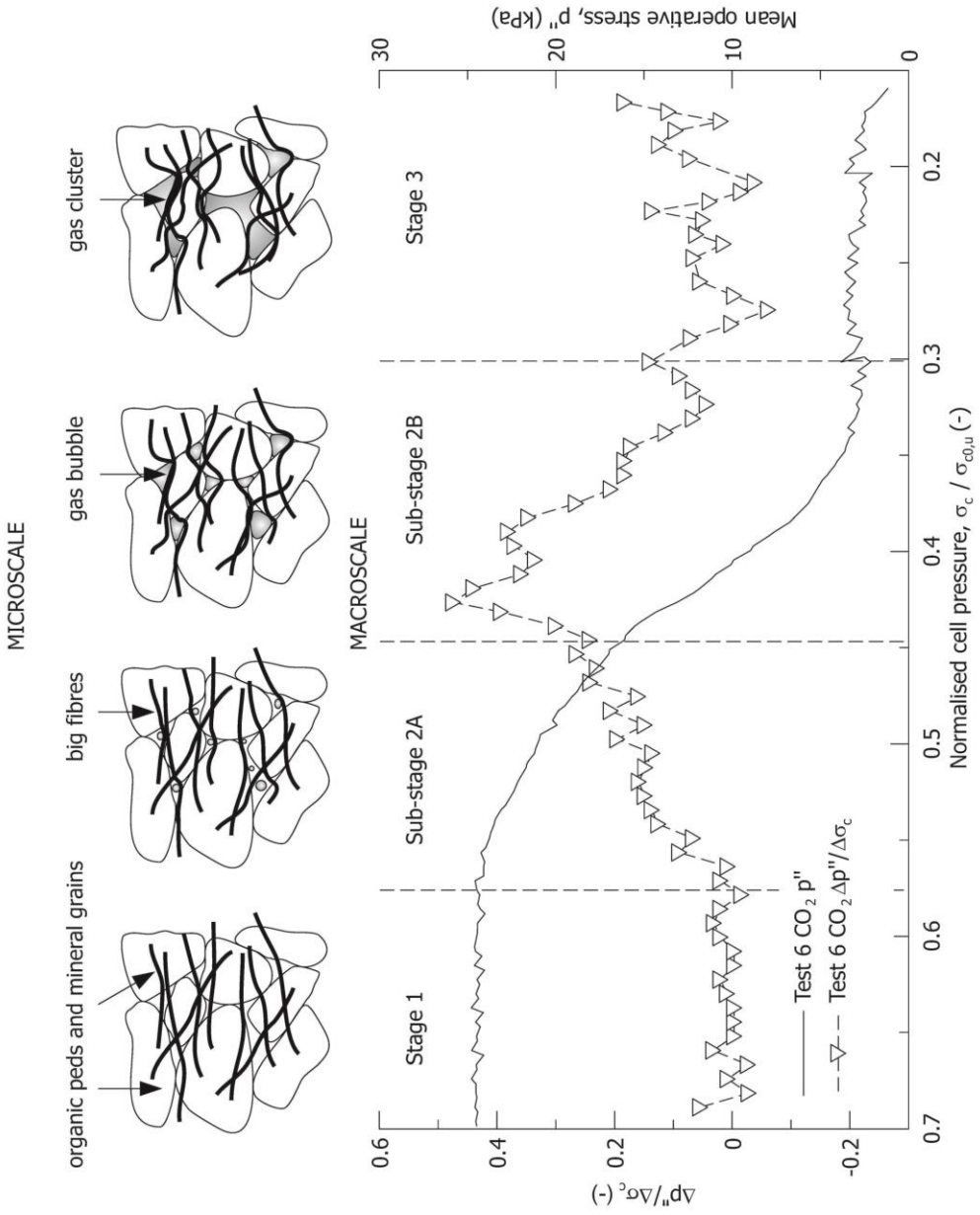

Jommi_Fig_11.jpg

Downloaded by [TU Delft Library] on [10/10/18]. Copyright © ICE Publishing, all rights reserved.

Accepted manuscript doi:
10.1680/jgeot.17.P.148

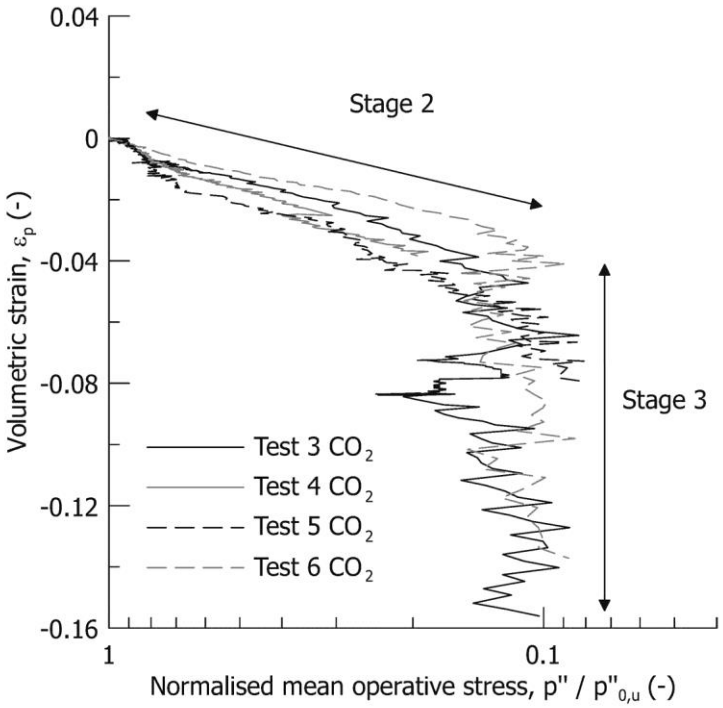

Jommi_Fig_12.jpg

Downloaded by [TU Delft Library] on [10/10/18]. Copyright © ICE Publishing, all rights reserved.

Accepted manuscript doi:
10.1680/jgeot.17.P.148

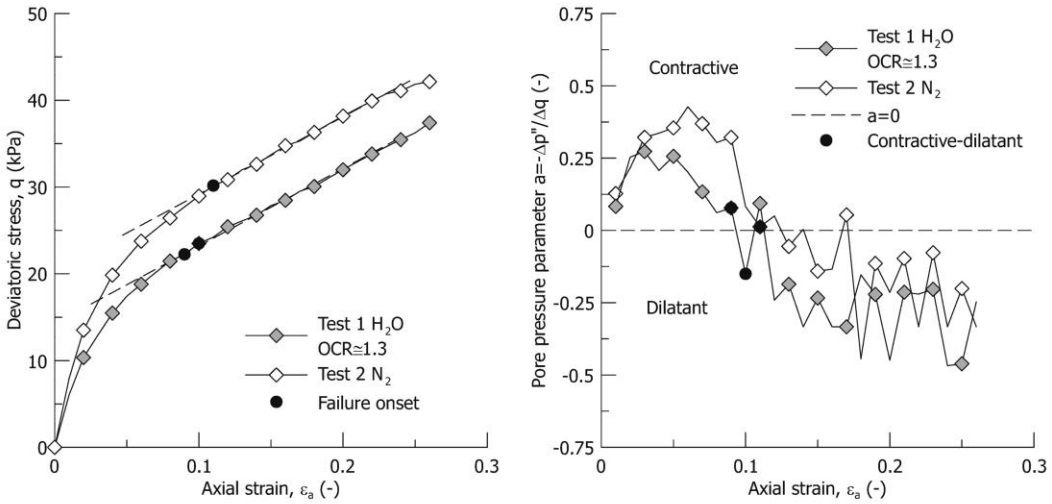

a) b)

Jommi_Fig_13.jpg

Downloaded by [TU Delft Library] on [10/10/18]. Copyright © ICE Publishing, all rights reserved.

Accepted manuscript doi:
10.1680/jgeot.17.P.148

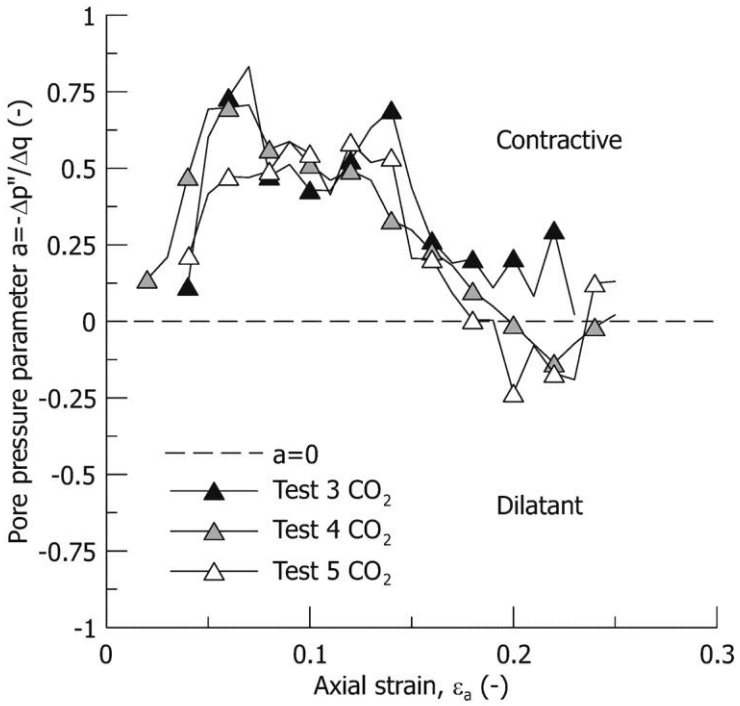

Jommi_Fig_14.jpg

Downloaded by [TU Delft Library] on [10/10/18]. Copyright © ICE Publishing, all rights reserved.

Accepted manuscript doi:
10.1680/jgeot.17.P.148

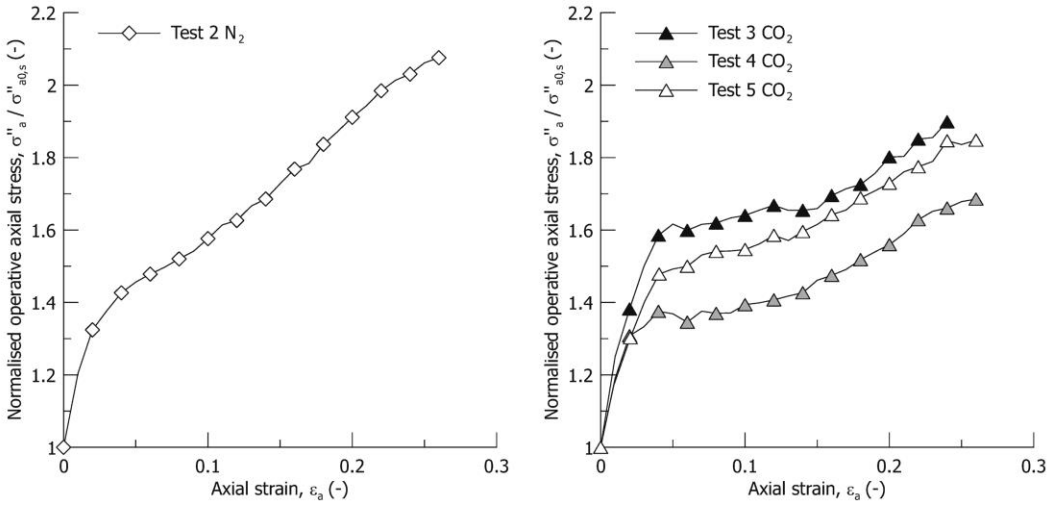

a) b)

Jommi_Fig_15.jpg

Downloaded by [TU Delft Library] on [10/10/18]. Copyright © ICE Publishing, all rights reserved.

Accepted manuscript doi:
10.1680/jgeot.17.P.148

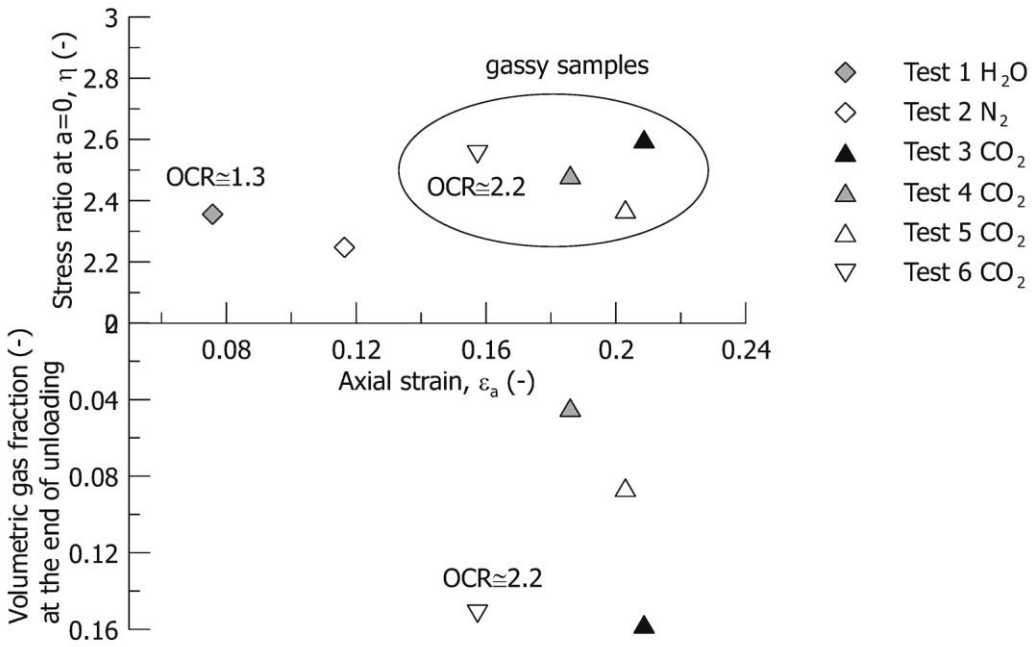

Jommi_Fig_16.jpg

Downloaded by [TU Delft Library] on [10/10/18]. Copyright © ICE Publishing, all rights reserved.

Accepted manuscript doi:
10.1680/jgeot.17.P.148

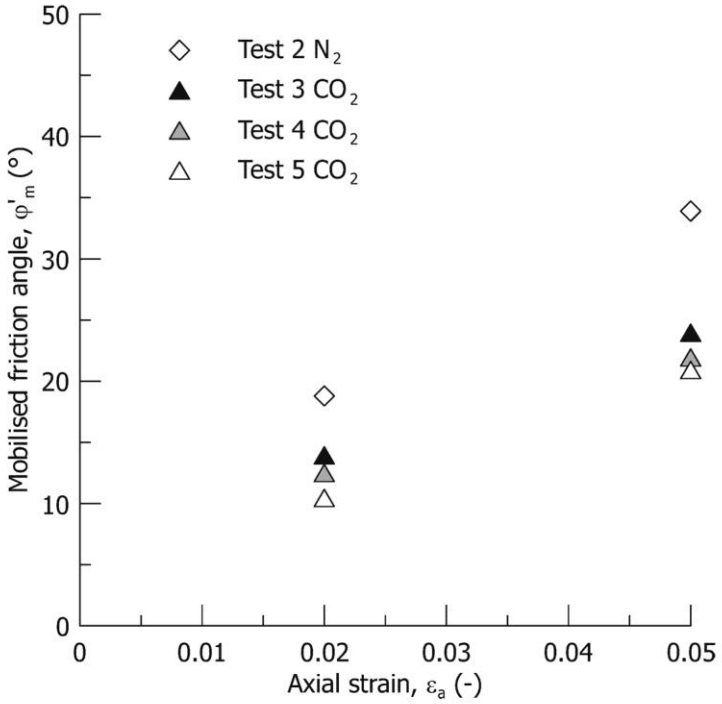

Jommi_Fig_17.jpg

Downloaded by [TU Delft Library] on [10/10/18]. Copyright © ICE Publishing, all rights reserved.